International Journal of Mass Spectrometry 276 (2008) 160–170

Contents lists available at ScienceDirect

International Journal of Mass Spectrometry

journal homepage: www.elsevier.com/locate/ijms

Charge-dependent dissociation of insulin cations via ion/ion electron transfer

Jian Liu, Harsha P. Gunawardena, Teng-Yi Huang, Scott A. McLuckey*

Department of Chemistry, Purdue University, 560 Oval Drive, West Lafayette, IN 47907-2084, USA

ARTICLE INFO

Article history:
Received 30 May 2008
Accepted 24 July 2008
Available online 3 August 2008

Keywords:
Electron transfer dissociation
Ion/ion reactions
Insulin mass spectrometry
Quadrupole/time-of-flight tandem mass spectrometry

ABSTRACT

The dissociation reactions of various charge states of insulin cations obtained directly from nano-electrospray were investigated as a result of ion/ion electron transfer from azobenzene anions. Data were collected with and without simultaneous ion trap collisional excitation of the first generation charge-reduced product during the ion/ion reaction period. Neither separation of the two constituent chains nor cleavages within the loop defined by the disulfide bridges were observed under normal electron transfer dissociation (ETD) conditions for any of the charge states studied. However, substantial sequence coverage (exocyclic region: 82.6%; entire protein: 38.8%) outside the ring structure was obtained for insulin +6, while only limited coverage (exocyclic: 43.5%; entire protein: 20.4%) was observed for insulin +5 and no dissociation, aside from low abundance side-chain losses, was noted for insulin +4 and +3 in the normal ETD spectra. When the first generation charge-reduced precursor ions were subjected to collisional activation during the ion/ion reaction period, higher sequence coverages were obtained for both insulin +5 (entire protein: 34.7%) and +4 (entire protein: 20.4%) with backbone cleavages occurring within the loop defined by the disulfide bonds. Dissociation of insulin +3 was not significantly improved by the additional activation. Separation of the two constituent chains resulting from cleavages of both of the two disulfide bridges that link the chains was observed for insulin +6, +5, and +4 when the charge-reduced species were activated. The dissociation of disulfide linkages in this study suggests that as the charge state decreases, disulfide bond cleavages dominate over N–Cα bond cleavages in the electron transfer dissociation process.

1. Introduction

Tandem mass spectrometry (MS/MS) plays a major role in protein identification and characterization [1,2]. In a typical MS/MS experiment, a precursor ion of interest derived from a protein/peptide is isolated and subsequently dissociated to produce (ideally) a range of product ions characteristic of the primary structure of the protein/peptide. The information that can be derived from a tandem MS experiment of a peptide or protein is a function of many factors, such as the dissociation approaches employed, the charge state and the nature of the precursor ion (e.g., protonated vs. metal cationized, open-shell vs. closed-shell, etc.), the modification state of the polypeptide, and so on. As for the dissociation method, collision-induced dissociation (CID) [3,4], in one form or another, is by far the most common approach and generally produces b- and y-type sequence ions from backbone amide bond cleavages. Electron capture dissociation (ECD) [5,6] is an alternative dissociation technique whereby an open-shell species is produced by the capture of a low-energy electron by a multiply charged polypeptide cation, which typically yields c- and z-type fragment ions through backbone N–Cα bond cleavages. ECD has proved to be particularly valuable in providing protein post-translational modification information and usually doing so with a wider range of backbone cleavages relative to CID. However, ECD is normally implemented in Fourier transform ion resonance cyclotron (FTICR) mass spectrometers, which operate under high vacuum conditions. With electron transfer being an ion/ion reaction analogue to electron capture, similar dissociation chemistry has been noted from the two phenomena. As a result, electron transfer dissociation (ETD) [7–9] shares many characteristics with ECD and has found increasing application in protein identification and characterization because of its compatibility with the widely used electrodynamic ion trap instruments.

The charge state of a protein or peptide cation has been shown to play an important role in the dissociation of both unmodified [10,11] and modified polypeptides, e.g., disulfide-linked peptides [12,13]. In the ETD reaction, for example, the peptide charge state has been found to affect significantly the competition between the various reaction channels [14]. As a result, the extent of dissociation and the variety of product ions differ substantially when the same polypeptide of different charge states is subjected to an ETD experiment [8]. A general observation has been made that as the polypeptide charge state decreases, the extent of dissociation and the variety of fragments produced in ETD decrease accordingly [14]. It has been

* Corresponding author. Tel.: +1 765 494 5270; fax: +1 765 494 0239.
E-mail address: mcluckey@purdue.edu (S.A. McLuckey).

1387-3806/$ – see front matter © 2008 Elsevier B.V. All rights reserved.
doi:10.1016/j.ijms.2008.07.028

demonstrated that when limited product ions were produced from an ETD reaction of polypeptide ions of low charge states, e.g., some triply and doubly charged tryptic peptides [15–17], activation of the charge-reduced precursor ions can be used to produce more sequence ions, as the charge-reduced precursor ions have been proposed to be consisting of c- and z-fragments remaining bound via non-covalent interactions [18] or comprising of an intact protein ion with a covalent bond significantly weakened by the electron attachment [19].

The modification state of a peptide or protein, such as the presence of disulfide linkages, can also play a major role in directing favored dissociation channels. Competition between the cleavages of disulfide linkages and backbone amide bonds has been observed in low-energy CID experiments. Multiply protonated species tend to show fragmentation of backbone bonds [20], whereas for singly charged species and negatively charged species, cleavages of the disulfide bond are the dominant channels [21]. Because of the lack of disulfide bond cleavage in many multiply protonated species, which can limit the primary sequence information from regions of the system that are protected by disulfide bonds, reduction of disulfide bridges prior to mass spectrometry is often performed [22]. On the other hand, both disulfide and backbone cleavages have been observed in ECD [23] and ETD [13,24] experiments, with preferred dissociation at the disulfide linkage. However, few systematic ECD or ETD studies have been focused on polypeptides of relatively large size with multiple disulfide linkages forming a ring structure in the molecule.

Many polypeptide species, such as insulin, have multiple disulfide linkages to stabilize the three-dimensional structure for proper biological function [25–27]. Due to the biological importance of insulin, the dissociation reactions of its gas-phase ions have been studied extensively [20,21]. With its three disulfide linkages, including two inter-chain disulfide linkages, insulin is an interesting system to explore the dissociation behavior of a whole protein possessing multiple chains linked by disulfide bridges. For this purpose, the charge-dependent dissociation behavior of insulin following an electron transfer event was investigated in this study under normal ETD conditions and by applying an external resonance excitation voltage to the first charge-reduced species during the course of ion/ion electron transfer reaction. The results provided here are likely to have important implications for the electron transfer dissociation of multiply disulfide-linked whole proteins in general.

2. Experimental

Bovine insulin and azobenzene were purchased from Sigma–Aldrich (St. Louis, MO) and used without further purification. Insulin was dissolved to 10 μM in 50/50/1 (v/v/v) methanol/water/acetic acid solutions for positive nano-electrospray ionization (nano-ESI) [28].

All experiments were performed on a commercial quadrupole/time-of-flight tandem mass spectrometer (Q-STAR XL, Applied Biosystems/MDS SCIEX, Concord, ON, Canada) modified to allow for ion/ion reactions [29]. A home-built pulsed dual source [30] was coupled directly to the interface of the Q-STAR instrument for the generation of ions of both polarities, which consists of a nano-ESI emitter for the generation of insulin cations and a corona discharge needle for atmospheric pressure chemical ionization (APCI) to generate azobenzene radical anions as the electron transfer reagents. Ion/ion electron transfer reactions were implemented in the Q2 quadrupole linear ion trap (LIT) in mutual storage mode, in which ions of opposite polarity were stored simultaneously by superposing an auxiliary radio frequency (rf) signal (250 kHz, 500 Vpp) on the end lenses (IQ2 and IQ3) to store ions in the axial direction, while normal operation of the oscillating quadrupole field of the Q2 quadrupole array stored ions of both polarities in the radial plane.

A typical scan function for the mutual storage mode electron transfer ion/ion reaction consists of the following steps: cation injection into Q2 LIT (50 ms), anion injection into Q2 LIT (300 ms), mutual storage of cations and anions in Q2 LIT (200 ms), and release of the ion/ion reaction products into the reflectron time-of-flight (TOF) for mass analysis (50 ms). For an ion/ion electron transfer reaction experiment, a positive high voltage (∼1400 V) applied to the nano-ESI emitter was first pulsed on to generate the insulin cations, which were sampled and transmitted into the mass spectrometer by properly adjusting the potentials on the ion optics via Daetalsyt 3.14, a version of research software developed by MDS SCIEX. The charge state of interest was isolated during its transmission through the Q1 quadrupole array, which was operated in the mass resolving mode. The analyte ions were cooled in the Q2 LIT for 30 ms with nitrogen as the buffer gas at a pressure of ∼5 mTorr, during which time the positive high voltage on the emitter was turned off. After this cooling step, a negative high voltage (∼2 kV) applied to the APCI wire was triggered on to generate the reagent anions, i.e., azobenzene radical anions in this study, which were subsequently transmitted into the Q2 LIT with a relatively low kinetic energy (∼5 eV) while Q1 was operated in the mass resolving mode. During this period, the dc potentials on the Q2 containment lenses were adjusted to a common value and set ∼0.5 V more positive relative to the Q2 rods while an auxiliary rf voltage was applied to the IQ3 lens. During the subsequent mutual storage step, the negative high voltage was turned off and a common dc potential was set for both the Q2 rods and the Q2 containment lenses. An auxiliary rf voltage was also applied to both of the Q2 containment lenses to enable the axial trapping of both polarities. After a specified mutual storage time, a positive dc potential was applied to the containment lenses to remove the residual reagent anions while the auxiliary rf voltage was terminated. In the final step, the positive ions consisting of the ion/ion reaction products and the unreacted precursor ions were released from Q2 LIT to the orthogonal reflectron TOF for mass analysis. To study the ion/ion electron transfer reaction with simultaneous activation of the first-generation charge-reduced precursor ions, an auxiliary dipolar ac frequency corresponding to the secular frequency of the charge-reduced ion was applied to one pair of the Q2 quadrupole rods during both the anion injection and subsequent mutual storage period while keeping other settings the same as in the mutual storage mode ETD experiments.

When an ion trap CID experiment was desired for a product ion derived from an ETD experiment, normal ion trap CID protocols were used after the product ion of interest generated in Q2 LIT was isolated in Q1 using a recently reported approach [31] through the bi-directional transfer of ions between Q2 and Q1 quadrupole arrays. Specifically, the entire positive ion population after the mutual storage period and the subsequent cooling step as discussed above were first transferred from the Q2 LIT to the Q1 quadrupole array, which is also operated as a LIT, by the employment of a combination of a negative LINAC [32,33] potential and a dc potential gradient decreasing from Q2 to Q1 along the ion optics. The product ion of interest can thus be isolated from the rest of ion population by operating Q1 in rf/DC mode after all the ions were accumulated in Q1. After the isolation, the dc potential of the Q1 quadrupole array was subsequently lifted along with the adjustment of dc potentials on the other ion optics between Q1 and Q2 so that an appropriate dc potential gradient along the ion optics can be generated to facilitate the transmission of the isolated ions from Q1 to Q2 LIT in a manner similar to that in the normal cation injection scenario. After the isolated product ion was accumulated

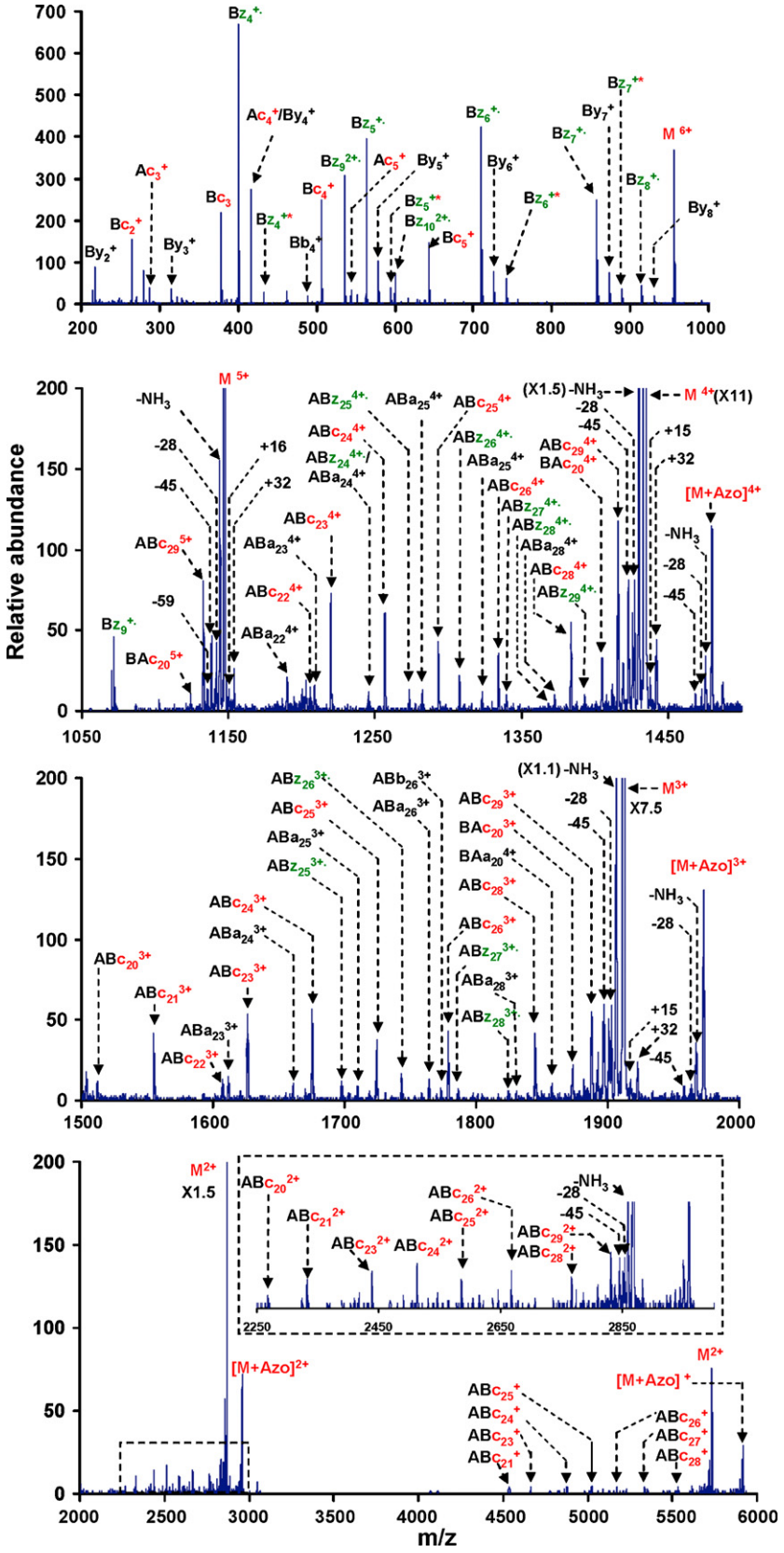

Fig. 1. Spectrum derived from normal ETD of insulin +6 charge state reacting with azobenzene radical anion. (z_n^{+*} denotes to oxygen adduct to z_n^+. $[M+Azo]^{m+}$ refers to the azobenzene adduct to the charge-reduced precursor ions. $-NH_3$, −28, −45 and −59 denote to the neutral losses. +15 and +32 are related to the oxygen adduct species from the corresponding charge-reduced precursor ions.).

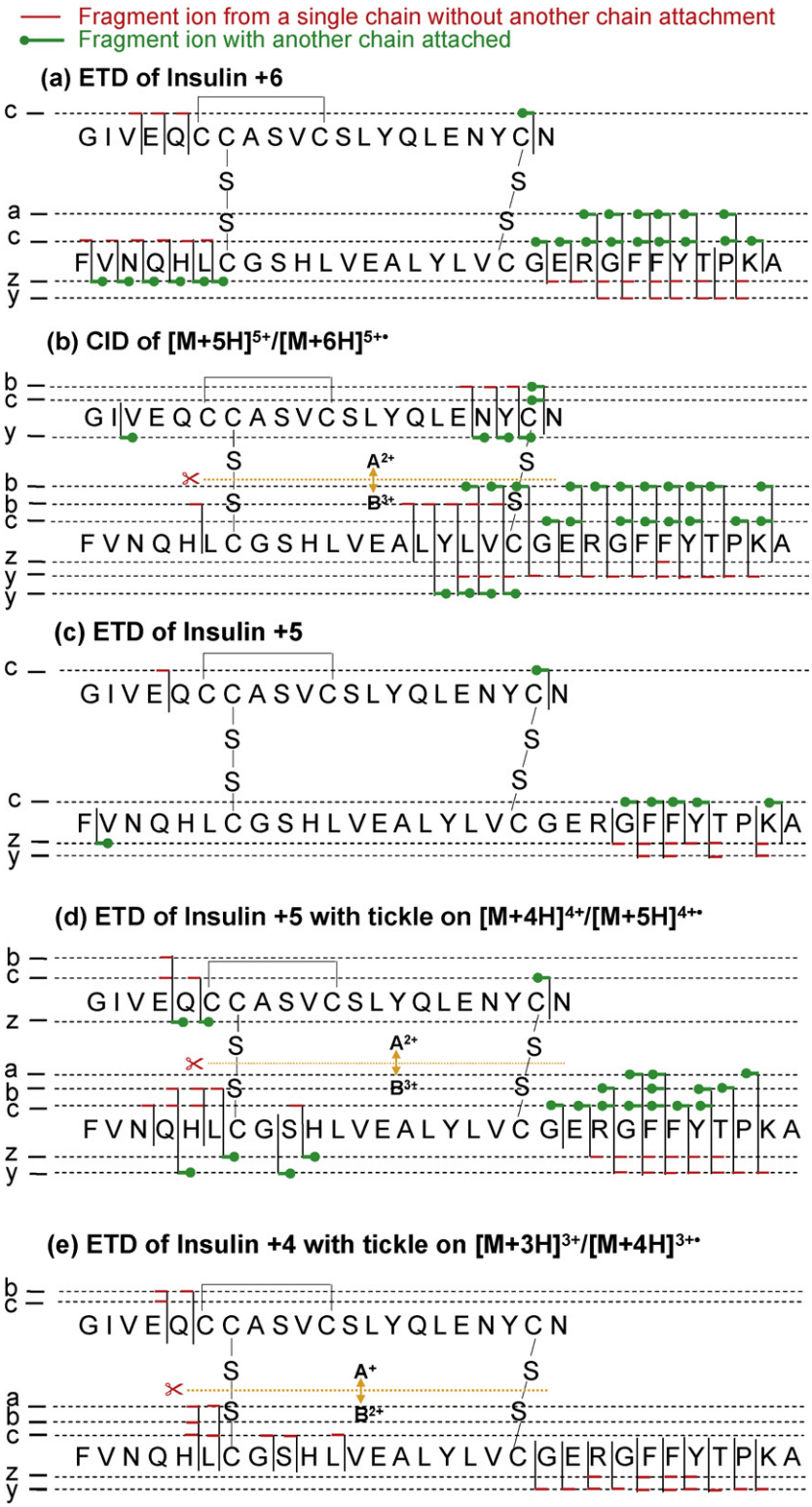

Scheme 1. Dissociation channels observed in (a) normal ETD of insulin +6 with azobenzene anions; (b) CID of $[M+5H]^{5+}/[M+6H]^{5+\bullet}$ derived from ETD of insulin +6 with azobenzene anions; (c) normal ETD of insulin +5 with azobenzene anions; (d) ETD of insulin +5 with azobenzene anions with a tickle on $[M+4H]^{4+}/[M+5H]^{4+\bullet}$ ions; (e) ETD of insulin +4 with azobenzene anions with a tickle on $[M+3H]^{3+}/[M+3H]^{3+\bullet}$ ions.

and cooled in Q2 LIT, ion trap CID can be performed by applying an appropriate auxiliary dipolar ac on one pair of the Q2 rods.

3. Results and discussion

3.1. Charge state-dependent fragmentation of insulin cations in normal ETD

Nano-ESI of bovine insulin under denaturing solution conditions gives rise to a distribution of charge states from +6 to +2. Dramatic differences in the fragmentation behaviors have been noted under normal ETD conditions, whereby protein cations react with reagent anions in a buffer gas without any additional ion activation. To relate the peptide backbone cleavages in this study, a notation of ABm_n is used to indicate a full A-chain attached to the B-chain which is cleaved so as to generate the m_n sequence ions. Alternately, BAm_n denotes to the cleavage of the A-chain to generate the m_n ions with the intact B-chain linked to it. For the sequence ions m_n produced from the cleavage of the A-chain without the attachment of the B-chain, a notation of Am_n is used, while the notation of Bm_n refers to the sequence ion m_n produced from the B-chain without attachment to the A-chain. Fig. 1 shows the ETD results for the insulin +6 charge state following reaction with the azobenzene radical anion, which is characterized by a wide range of c- and z-type fragments along with abundant charge-reduced precursor ions. In the m/z region lower than the precursor ion ($m/z < 950$), fragment ions of the highest relative abundance were produced, most of which were singly charged c- and z-ions formed from parts of the A-chain and B-chain that fall outside the ring defined by the two disulfide linkages and the portions of the chains they encompass. These small fragment ions (Ac_3^+–Ac_5^+, Bc_2^+–Bc_6^+, Bz_4^+–Bz_8^+, Bz_9^{2+} and Bz_{10}^{2+}) together with the Bc_1^+ and Bz_2^+ ions (the latter of which are not shown in Fig. 1 but were observable when a lower Q2 low mass cut-off was used in the ion/ion reaction experiment) covers 73.9% of the exocyclic sequence (17 cleavages/23 bonds) and 34.7% of the whole protein (Scheme 1(a)). There exists a complete set of c- and z-ions (ABz_{24}–ABz_{29}, ABc_{20}–ABc_{26} and ABc_{28}) in the high m/z region of the spectrum that are complementary to all the small c- and z-ions (Bc_1–Bc_6, Bz_2 and Bz_4–Bz_{10}) observed in the low mass region from the B-chain. A total of fourteen c/z-ion complementary pairs are represented in this ETD experiment for the insulin +6. Most of the large c-fragment ions from the B-chain appear over the range of charge states from +4 to +1 in the high m/z region of the spectrum ($m/z > 1000$). On the other hand, the majority of large z-fragments from the B-chain, with much lower abundance relative to the c-fragments, were mostly quadruply and triply charged, which is likely due to relatively lower detection efficiencies for the high m/z ions.

In addition to the characteristic c- and z-product ions, a- and y-type ions are also common ETD products. Such ions were also noted in this study, as reflected by the appearance of a series of multiply charged a-ions (ABa_{22}–ABa_{26} and ABa_{28}) as well as a set of contiguous y-ions (By_2^+–By_8^+) of low relative abundance from the B-chain C-terminal region. Another common set of reactions in ETD result in the loss of small neutral fragments from amino acid side chains, which are denoted in the spectra as "$-NH_3$", or "−28", "−45", and "−59", the latter numerical values representing the masses of the lost neutrals which correspond to losses of CO, side chain of asparagine, and side chain of arginine, respectively. These neutral losses were apparent in the ETD results of all insulin charge states. The attachment of oxygen present in the vacuum system to radical ions formed via ion/ion electron transfer noted previously [34] was also observed here. For example, all the charge-reduced precursor ions, as well as the z_4^+–z_8^+ ions, formed adducts with the background oxygen in the ion trap, with the former also giving another adduct of $[M+O-H+mH]^{m+}$, which arises via $OH^\bullet$ loss from the oxygen adduct. Another major adduct formed in this study is the complex between the charge-reduced precursor ion and the azobenzene anion, denoted as $[M+Azo]^{m+}$ in Fig. 1. The attachment of the reagent anion to a cation is not common in ETD for small peptides. The appearance of this azobenzene adduct is presumably due to the large relative size of the insulin protein cations under investigation, which significantly increases the cross-section for complex formation [35]. The data of Fig. 1 reveal that dissociation of the insulin backbone is preferred near the C-terminus of the B-chain, as suggested by the existence of a variety of relatively abundant a-, y-, c-, and z-ions. As shown in Scheme 1(a), no backbone cleavages are apparent from within the loop structure defined by the two inter-chain disulfide bonds, which would require the cleavage of at least two bonds. No evidence for separation of the A- and B-chains is apparent either, which would also require cleavage of at least two bonds. However, the c- and z-ions derived from this ETD reaction gives almost complete sequencing of the structure outside the loop (19 out of 22 possible cleavages). As a result, the total sequence coverages obtained from ETD of insulin +6 are 82.6 and 38.8% for the exocyclic portion and for the whole protein, respectively.

Fig. 2 shows the normal ETD results derived from ion/ion reaction between the insulin +5 charge state with azobenzene radical anions. Similar to the results for the +6 charge state, there is no evidence for the separation of the two chains and cleavages from within the cyclic structure. Also, the most abundant c- and z-fragment ions are the singly charged low mass ions derived largely

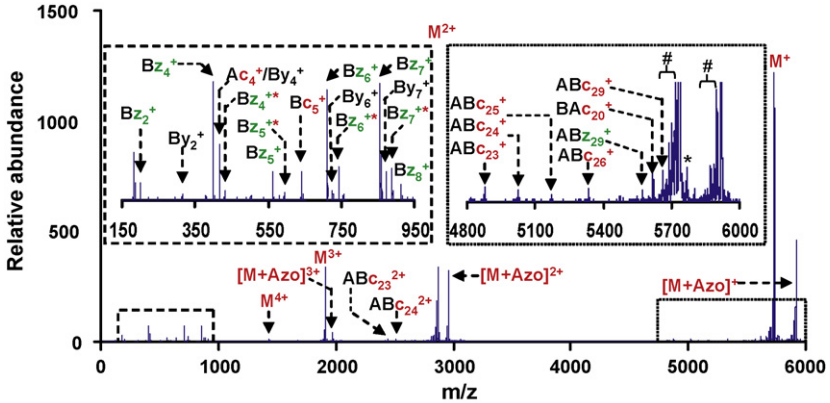

Fig. 2. Spectrum derived from normal ETD of insulin +5 charge state reacting with azobenzene anions. ('#' denotes neutral losses. '*' refers to oxygen adducts. $[M+Azo]^{m+}$ refers to azobenzene adduct to the charge-reduced precursor ions. The same notations are used in the spectra below.).

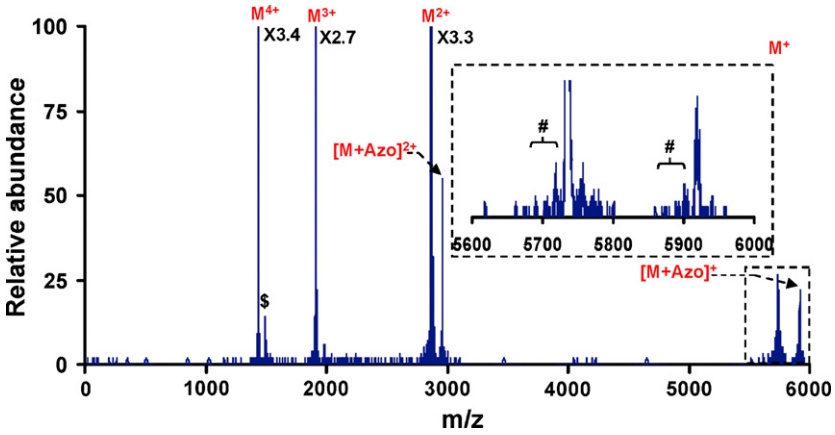

Fig. 3. Spectrum derived from normal ETD of insulin +4 charge state reacting with azobenzene anions. ('$': species from isolation).

from the C-terminus of the B-chain. However, the variety and the relative abundances of the product ions derived from the +5 charge state are much lower than those derived from the +6 charge state, with only 2 c-ions from the A-chain, and 5 c-ions, 7 z-ions and 4 y-ions from the B-chain being observed. As a result, backbone cleavages cover only 43.5% of the sequence outside the cyclic structure and 20.4% of the whole protein (Scheme 1(c)). Furthermore, only 4 c/z-ion pairs were generated for the protein and these were exclusively from the C-terminus of the B-chain. The ETD results obtained here differ from previous data [23] collected via ECD on the +5 charge state of insulin. Two major differences were noted between the two experiments, i.e., (i) the dominant separation of the two constituent A- and B-chains in ECD, which required cleavage of both of the two inter-strand disulfide linkages, and (ii) the production of a Bz_{15} ion from ECD within the ring, which required the cleavage of an N–Cα bond and the disulfide bond between A-chain Cys-20 and B-chain Cys-19.

Neither of the two-bond cleavage products is noted in the ETD results. Furthermore, slightly higher sequence coverage was obtained in the ECD of insulin +5 charge state than in ETD of the same charge state. The difference observed between these two techniques perhaps can be accounted for by the fact that ECD is more exothermic than ETD. The exothermicity associated with ECD is the negative of the recombination energy of the protein cation, and is higher than that associated with the ETD by a value equal to the electron affinity of the neutral species used to form the reagent anion. Furthermore, all of the reaction exothermicity is expected to appear as internal energy of the electron capture product ion in the case of ECD, whereas some of the reaction exothermicity in ETD can be partitioned into translational and internal modes of the neutralized reagent.

The dramatic effect of precursor ion charge state on the dissociation of insulin cations under normal ETD conditions is clearly apparent when the results from +6 charge state (Fig. 1) are compared with those from insulin +4 charge state (Fig. 3). In contrast to the production of a variety of fragment ions in +6 charge state case, no abundant dissociation products, other than small neutral losses, were observed in the normal ETD of +4 charge state. The major ETD products are the charge-reduced precursor ions along with their complex ions with azobenzene. Similar to +4 charge state, normal ETD of the insulin +3 charge state did not give any dissociation products except some neutral loss products of very low abundance (data not shown). This observation is consistent with results from studies of non-disulfide-containing peptides [14], in which increased relative contributions from neutral losses are observed with the decrease of the charge state of the same peptide.

The increase in both the number of dissociation channels and the total abundance of dissociation products with insulin charge state is consistent with previous observations of the ETD of unmodified polypeptide ions [14] and linear disulfide-linked peptide cations [13]. Several factors can contribute to this general tendency. For example, reaction exothermicity increases with cation charge state via an increase in recombination energy. For polypeptide cations, an average increase of 1.1 eV/charge in ionization energy has been reported [36], which would also be reflected in the ion recombination energy for polypeptide cations. A second factor is the lower kinetic stabilities associated with more highly charged product ions. The first generation charge-reduced species from more highly charged precursor ions have greater degrees of internal electrostatic repulsion, which can facilitate dissociation. Furthermore, the electrostatic repulsion within the precursor ion may also play a role in determining which sites in the ion can capture an electron, which is discussed further below. There is also likely to be an important role for precursor ion charge state in determining the extent to which proton transfer competes with electron transfer as an ion/ion reaction mechanism.

3.2. CID on the charge-reduced precursor ion of $[M+5H]^{5+}/[M+6H]^{5+\bullet}$

Abundant intact charge-reduced products are common to the ETD spectra for all of the insulin charge states examined here (i.e., +6 to +3), which can be comprised of mixtures of products from proton transfer and electron transfer. Charge-reduced protein species formed from electron capture have been proposed to consist of c/z-fragments remaining bound via non-covalent interactions [18] or, alternatively, as an intact protein ion with a covalent bond significantly weakened by the electron attachment [19]. In either case, subsequent activation of the charge-reduced product can lead to more ECD- or ETD-like products. The electron transfer product component in the charge-reduced precursor ions (ET, no D) of non-disulfide-linked peptide ions and a linear disulfide-linked peptide ion have been activated to provide additional ETD products [15–17], which, in some cases, provided sequence information complementary to that obtained in normal ETD. To probe the nature of the charge-reduced precursor ion produced from a protein ion with an intramolecular cyclic structure formed by multiple inter-chain disulfide linkages, the charge-reduced species generated in ETD reaction of insulin +6 with azobenzene radical anions, $[M+5H]^{5+}/[M+6H]^{5+\bullet}$, were isolated and subjected to ion trap CID in Q2.

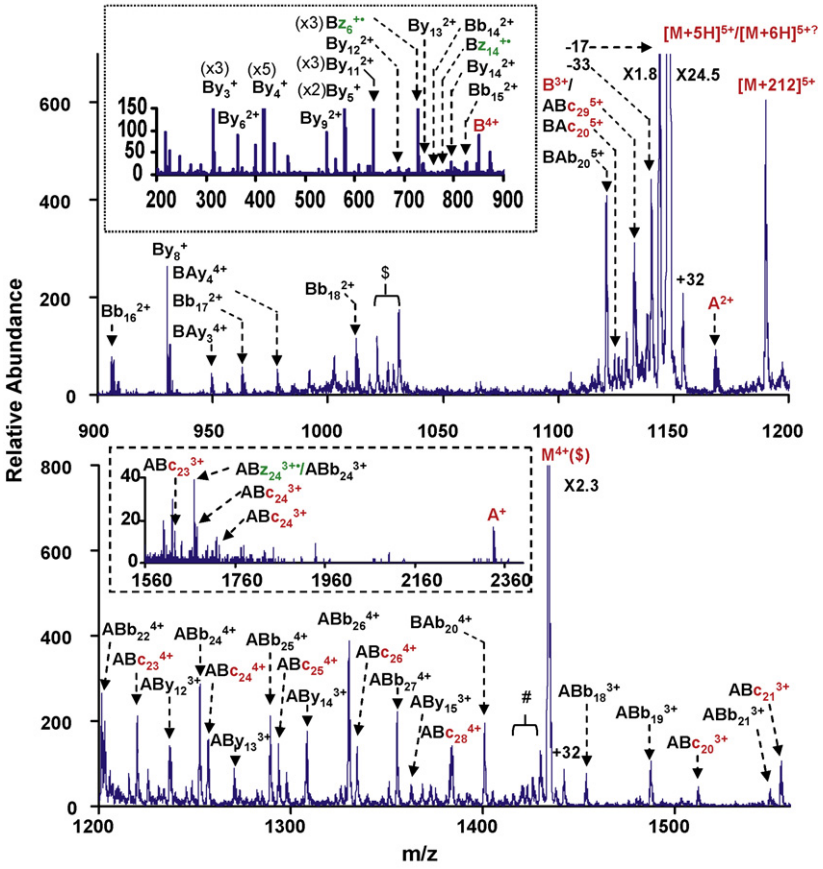

Fig. 4. Spectrum derived from CID (frequency: 64.3 kHz, amplitude: 300 mVpp) of the charge-reduced precursor ion, $[M+5H]^{5+}/[M+6H]^{5+\bullet}$, produced from ETD of insulin +6 with azobenzene anions.

The CID results, which are provided in Fig. 4, show a combination of c/z-, and b/y-type product ions, with the latter being the major products under the CID conditions used. The majority of fragments come from the C-terminal region of the B-chain, such as a contiguous series of y-type ions, By_2–By_{14}, that reflect the sequence LVCGERGFFYTP (Scheme 1(b)). In spite of their low abundance, three of the y-type ions from this sequence, By_{12}^{2+}–By_{14}^{2+}, can be readily identified by the corresponding isotope envelopes and are clearly distinguishable from the background noise. These fragments arise from cleavages within the ring comprised of the inter-chain disulfide bridges and the portion of the two chains within the disulfide linkages. Thus, the presence of these ions indicates the cleavage of a peptide bond and the disulfide bond linking the A-chain Cys-20 and B-chain Cys-19. The complements of ten of thirteen of these y-ions (By_2–By_{14}) are apparent (viz., ABb_{17}–ABb_{19}, ABb_{21}–ABb_{27}) all of which contain the intact A-chain. Two of these ions, ABb_{17} and ABb_{18}, are products of cleavages from within the ring structure with each requiring cleavages of an amide bond and the disulfide linkage between A-chain Cys-20 and B-chain Cys-19. Previous collisional activation studies of the insulin $[M+5H]^{5+}$ ion do not show products from cleavages within the ring structure [20]. This strongly suggests that the fragment products arising from dissociation from within the ring structure come from the ET, no D component in the charge-reduced precursor ions. It is also apparent that there are at least five cleavages from within the ring structure that give rise to Bb-type ions (Bb_{14}–Bb_{18}), which correspond to cleavages of the LYLV residues in the B-chain. Of these 5 ions, four have ABy-type complementary ions (ABy_{12}–ABy_{15}) indicating the cleavage of the inter-chain S–S bond between A-chain Cys-7 and B-chain Cys-7. In addition to the two exocyclic cleavages giving the BAy_{19} and BAb_{20} fragments, backbone cleavages of the A-chain were also observed within the ring structure, which yielded three contiguous product ion pairs (Ab_{17}/BAy_4, Ab_{18}/BAy_3, and Ab_{19}/BAy_2). These fragments, as well as those from cleavages in the B-chain between the residues LYLVC, suggest that electron transfer to the $[M+6H]^{6+}$ ion cleaved one or the other of the inter-chain disulfide bonds and that subsequent collisional activation cleaved amide bonds. This is a more likely scenario than ETD of the backbone followed by CID of the disulfide bond because such a process would likely yield c/z-type ions.

Collisional activation of the charge-reduced ions also leads to separation of the A- and B-chains. Separated chains are not observed in the direct ETD of the +6 precursor and ion trap collision-induced dissociation of the $[M+5H]^{5+}$ ion shows no evidence for chain separation. This strongly suggests that the $[M+6H]^{5+\bullet}$ species is the origin of the separated chains. Nominally two sets of complementary products are observed; viz., $(B\text{-chain})^{4+}/(A\text{-chain})^{+}$ and $(B\text{-chain})^{3+}/(A\text{-chain})^{2+}$. However, careful examination of the isotopic compositions of the various chain-related ions reveals that there is a mixture of products for each charge state partitioning. Scheme 2 summarizes schematically four of the eight possible complementary pairs for the $(B\text{-chain})^{4+}/(A\text{-chain})^{+}$ charge partitioning. Previous examination of two peptide chains linked by a single disulfide bond showed that CID of the protonated species results in the transfer of a hydrogen atom from one chain to the other upon cleavage of the disulfide bond where as ETD of the doubly protonated species lead to a radical site on one chain and the thiol on the other

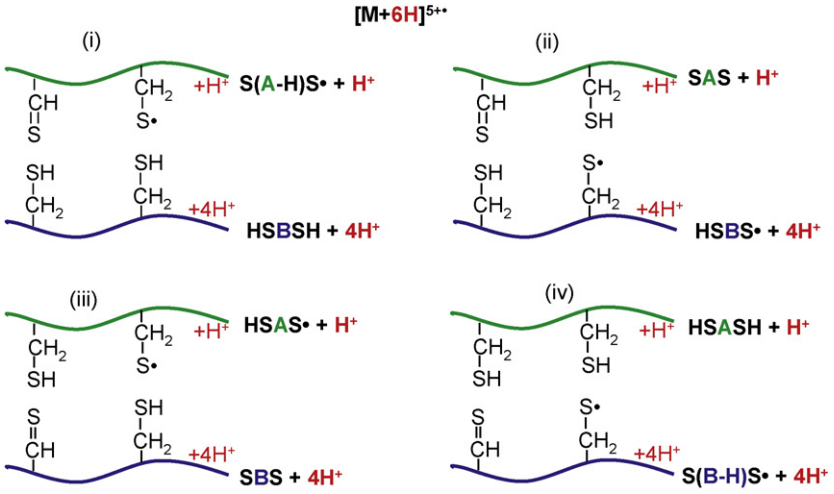

Scheme 2. Schematic depiction of the various complementary A-chain and B-chain fragments from collisional activation of the $[M+6H]^{5+\bullet}$ ion of insulin.

chain [13]. Scheme 2 shows the two possible hydrogen transfer possibilities for the left-most disulfide linkage and the two radical site possibilities for the right-most disulfide linkage. Four other possibilities exist for the reverse cases (i.e., ETD of the left-most disulfide linkage and CID of the right-most disulfide linkage). The $(B\text{-chain})^{4+}/(A\text{-chain})^{+}$ charge combination, for example, includes the $[HSBSH+4H]^{4+}/[S(A–H)S^{\bullet}+H]^{+}$, $[HSBS^{\bullet}+4H]^{4+}/[SAS+H]^{+}$, $[SBS+4H]^{4+}/[HSAS^{\bullet}+H]^{+}$, and $[S(B–H)S^{\bullet}+4H]^{4+}/[HSASH+H]^{+}$ complementary pairs (as well as the corresponding complementary pairs with the radical site located on the left-most disulfide). These combinations are consistent with initial ETD of one of the disulfide bonds giving rise to a charge-reduced $[M+6H]^{5+\bullet}$ ion with one remaining intact inter-strand disulfide bond that subsequently is fragmented via CID.

Interestingly, the Bb-type ions from the cleavage within the cyclic structure (viz., Bb_{14}–Bb_{18}) are mostly odd-electron species (i.e., the radical site likely originating on the B-chain Cys-7, Bb(S•)). A minor contribution from even-electron species Bb(SH) may also be present. The radical ions are likely to be formed from initial ETD of the A-chain Cys-7/B-chain Cys-7 inter-strand linkage with radical site retention on the B-chain followed by CID to yield the radical Bb-type ions (see Scheme 3). There are a few c- and z-type ions in the CID data of the charge-reduced species, which primarily arise from the C-terminus of the B-chain. In all cases, these ions arise from cleavages outside the loop defined by the two inter-strand disulfide linkages. For these products, the initial electron transfer event serves to cleave or weaken N–Cα bonds of the peptide, rather than cleave one of the disulfide linkages. The direct ETD of the $[M+6H]^{6+}$ ion (see Fig. 1 and Scheme 1(a)) and these products clearly show that electron transfer to the peptide backbone and to the disulfide linkages are competitive processes for the +6 ion.

3.3. Charge-dependent ETD of insulin cations with simultaneous excitation on the first charge-reduced precursor ions

To improve the low production of ETD products in the ion/ion electron transfer to insulin cations of the lower charge states, i.e., +5, +4, and +3, simultaneous activation of the first charge-reduced precursor ions can be performed during the course of an ETD reaction by the application of an external resonant excitation. The ETD spectrum obtained by this approach is shown in Fig. 5 for the insulin +5 charge state, which gives higher sequence coverage (28.6%) via ETD (through production of a greater variety of c- and z-ions) than that (20.4%) under normal ETD conditions. The number (24) of c/z-ions (Scheme 1(d)) produced with collisional activation of the initially formed charge-reduced species during the ion/ion reaction period almost doubled that (14) (Scheme 1(c)) in the normal ETD experiment, yielding more complementary c/z-ion pairs (9 pairs) as comparing to that (4 pairs) produced in normal ETD, including one pair (Bc_9^{+}/ABz_{21}^{3+}) from the cleavage within the ring structure. The major production of c/z-ions occurs from both C- and N-termini of the B-chain, in contrast to arising mostly from the C-terminal end of the B-chain in the case of the normal ETD experiment. In addition, six b/y-complementary ion pairs were also produced from the cleavage of B-chain amide bonds as a result of the supplementary vibrational activation. Separation of the two chains is also a major process in the supplementary activation experiment, whereas it is not observed from the direct ETD experiment. Relatively small signals that show cleavages of the carbon–sulfur bonds of the disulfide linkages is also apparent, which has been noted before in the collisional activation of disulfide-linked species [20].

The benefits from activating the charge-reduced precursor ions during an ETD process are clearly reflected in the case of the insulin

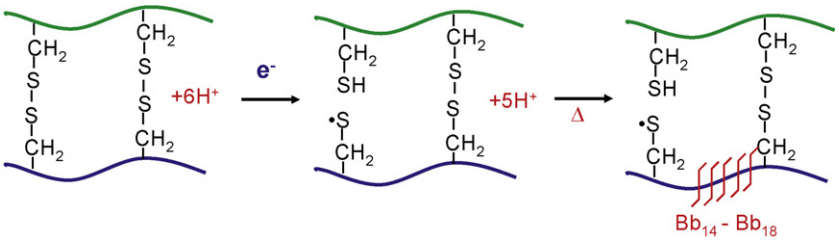

Scheme 3. Schematic depiction of a two-step process involving ETD and CID to generation odd-electron Bb_{14}–Bb_{18} ions from electron transfer to insulin $[M+6H]^{6+}$ followed by CID of $[M+6H]^{5+\bullet}$.

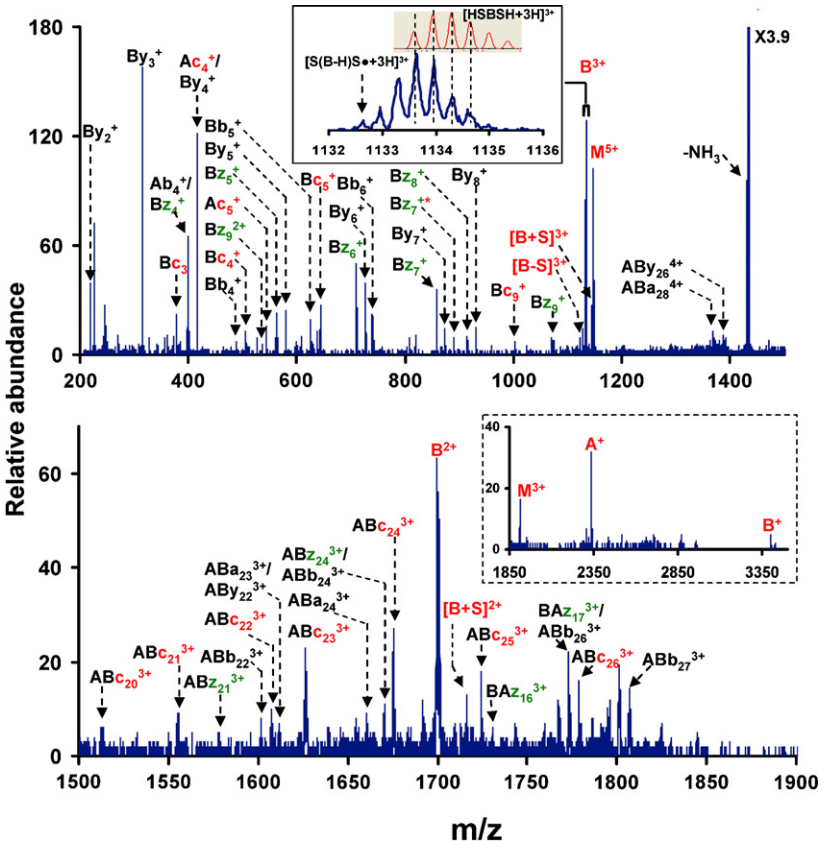

Fig. 5. Spectrum derived from ETD of insulin +5 with azobenzene anion with simultaneous excitation (560 mV, 52.31 kHz) on $[M+4H]^{4+}/[M+5H]^{4+\bullet}$ during the course of ion/ion reactions.

+4 charge state, for which no c- and z-fragments or ions from the individual chains were observed under normal ETD conditions (Fig. 3). The activation of the ET, no D component, $[M+4H]^{3+\bullet}$, from this reaction yielded one c-ion (Ac_4^+) from the A-chain, 5 c-ions (Bc_5^+, Bc_6^+, Bc_8^+, Bc_9^+ and Bc_{11}^+) and 4 z-ions (Bz_5^+–Bz_7^+ and Bz_9^+) from the B-chain, and, as a result, a sequence coverage of 20.4%. Among the 5 Bc-type ions produced in the N-terminal region of the B-chain, three ions (Bc_8^+, Bc_9^+ and Bc_{11}^+) were from dissociation from within the ring structure. Also, there is a series of small By-type ions (By_2–By_{11}) generated as CID products, reflecting the sequence GERGFFYTP. As with the other collisionally activated charge-reduced ions, the $[M+4H]^{3+\bullet}$ species showed a strong tendency for chain separation. In fact, based on the relative signal strengths of the separated chains versus the total c- and z-ion signals, most of the electron transfer to the $[M+4H]^{4+}$ ion cleaved disulfide bonds rather than N–Cα bonds (see below).

When insulin +3 was subjected to ETD, significant improvement in the production of neither c/z-product ions nor separated chain ions was observed with the simultaneous excitation of the charge-reduced precursor ions in the ion/ion reaction period (data not shown). Essentially no ions from the separated chains, c/z-, or b/y-type fragment ions were observed in the experiment. Rather,

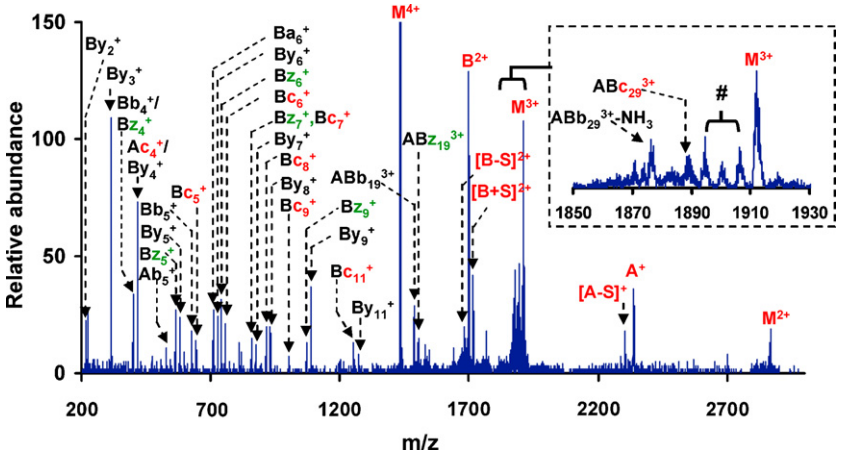

Fig. 6. Spectrum derived from ETD of insulin +4 with azobenzene anions with simultaneous excitation (320 mV, 38.6 kHz) on $[M+3H]^{3+}/[M+4H]^{3+\bullet}$ during the course of ion/ion reactions.

small neutral losses, such as ammonia loss, were observed. This may be due to proton transfer dominating over electron transfer in the ion/ion reaction of this low charge state, thereby yielding primarily the $[M+2H]^{2+}$ ion. The insulin $[M+2H]^{2+}$ species is known to give rise small neutral losses under ion trap CID conditions [20]. However, it is also possible that electron transfer to the low charge state insulin ion localizes the electron at the protonation sites, which then fragment via small neutral losses from the side-chain.

It is noteworthy that collisional activation of the charge-reduced ions $[M+5H]^{4+\bullet}$ and $[M+4H]^{3+\bullet}$ show chain separation as the dominant class of fragmentation pathways, as indicated by the B^{3+}, B^{2+}, B^{+} and A^{+} ions in Fig. 5 and B^{2+} and A^{+} ions in Fig. 6, respectively. Close examination of the isotope peaks associated with these ions reveals that they are a mixture of complementary products, in analogy with the situation discussed for the $[M+6H]^{5+\bullet}$ ion (see Scheme 2). The fractional contribution of chain separation relative to backbone cleavages increases in the order $[M+4H]^{3+\bullet} > [M+5H]^{4+\bullet} > [M+6H]^{5+\bullet}$. A similar tendency has been noted in the direct ETD of model disulfide-linked peptides in which the more highly charged ions showed higher relative contributions from N–Cα bond cleavage [24]. This observation can be rationalized if one of the variations of the "Coulomb assisted" dissociation models put forward by Turecek et al. and Simons et al. [37–39] hold. According to a direct attachment version of the proposed mechanism, the electron can attach directly to the OCN amide π^* orbital, leading to N–Cα bond cleavage, or a S–S σ^* orbital, to effect disulfide bond cleavage. A variation of this picture is initial electron attachment to a Rydberg orbital of a protonation site with electron transfer to one of the anti-bonding orbitals. However, vertical electron attachment or electron transfer to the OCN amide π^* or S–S σ^* orbitals without Coulomb stabilization is approximately 2.5 and 1 eV endothermic [39], respectively. Less Coulomb stabilization is required to render exothermic electron attachment/transfer to the S–S σ^* orbital than to the OCN amide π^* orbital. Hence, the tendencies for N–Cα bond cleavage and for S–S bond cleavage via ETD can be expected to show different charge state dependencies in that the likelihood for N–Cα bond cleavage can be expected to show a faster drop-off with precursor ion charge. Whatever the underlying reason may be, recognizing that there is a different precursor charge dependence for N–Cα bond cleavage than for S–S bond cleavage is important in the selection of precursor ion charge states for the ETD of disulfide-linked peptides and proteins. If N–Cα bond cleavage is desirable, for example, it is important to select high charge states to maximize Coulomb stabilization. However, if it is desirable to maximize selectivity for disulfide bond cleavage, the selection of somewhat lower precursor ion charge states may be warranted to minimize contributions from N–Cα bond cleavages while retaining the ability to cleave the disulfide bond.

4. Conclusions

Significant differences have been observed in the dissociation behaviors of various charge states of insulin cations from +6 to +3 charge states produced directly from nano-ESI, when subjected to electron transfer reactions with the azobenzene radical anion. No evidence for separation of the constituent A- and B-chains and cleavages within the ring structure defined by the two inter-chain disulfide linkages and the portions of the chains enclosed by them has been observed in the normal ETD of any of the charge states investigated. However, almost complete sequence coverage (82.6%) of the exocyclic portion of the protein (38.8% coverage for the whole protein) has been obtained in the normal ETD of insulin +6, in which ETD was performed without additional excitation to the products ions during the course of reaction. Only limited sequence coverage (20.4% of the whole protein) was obtained for normal ETD of insulin +5 and no dissociation was observed for insulin +4 and +3 under normal ETD conditions. When the charge-reduced species, $[M+5H]^{5+}/[M+6H]^{5+\bullet}$, derived from ETD of insulin +6 with azobenzene anions were subjected to ion trap CID, extensive c- and z-ions were observed along with some b/y-type complementary ion pairs corresponding to the cleavages within the ring structure, in addition to the fragment ions related to the separation of the A- and B-chains. When the charge-reduced precursor ions were simultaneously activated during the course of ion/ion electron transfer reactions, cleavages of both inter-chain disulfide linkages and dissociations within the ring structure were observed for insulin +5 and +4 ions. Furthermore, higher sequence coverages were obtained for insulin +5 (34.7%) and +4 (20.4%) than the sequence coverage from the same charge state obtained under normal ETD conditions. The results described here also show that the charge state dependencies of N–Cα bond cleavage and S–S bond cleavage upon electron transfer ion/ion reaction do not closely mirror one another. That is, the tendency for N–Cα bond cleavage falls off more quickly with insulin charge state than does S–S bond cleavage. This tendency is consistent with the Coulomb assisted electron attachment/transfer mechanisms proposed by the Simons et al. and Turecek et al.

Acknowledgments

This work was supported by the US Department of Energy, Office of Basic Energy Sciences, Division of Chemical Sciences under Award No. DE-FG02-00ER15105. The authors acknowledge Dr. Frank Londry, Dr. Bruce Thompson, Dr. Jim Hager, and Dr. Mahmoud Risheri of MDS SCIEX for help with the instrumentation and Dr. Min Yang of MDS SCIEX for providing custom instrument control software.

References

[1] K.R. Jennings, Int. J. Mass Spectrom. 200 (2000) 479.
[2] R. Aebersold, D.R. Goodlett, Chem. Rev. 101 (2001) 269.
[3] S.A. McLuckey, D.E. Goeringer, J. Mass Spectrom. 32 (1997) 461.
[4] D.F. Hunt, J.R. Yates, J. Shabanowitz, S. Winston, C.R. Hauer, Proc. Natl. Acad. Sci. U.S.A. 83 (1986) 6233.
[5] R.A. Zubarev, N.L. Kelleher, F.W. McLafferty, J. Am. Chem. Soc. 120 (1998) 3265.
[6] R.A. Zubarev, Mass Spectrom. Rev. 22 (2003) 57.
[7] J.E.P. Syka, J.J. Coon, M.J. Schroeder, J. Shabanowitz, D.F. Hunt, Proc. Natl. Acad. Sci. U.S.A. 101 (2004) 9528.
[8] S.J. Pitteri, P.A. Chrisman, J.M. Hogan, S.A. McLuckey, Anal. Chem. 77 (2005) 1831.
[9] J.J. Coon, J.E.P. Syka, J.C. Schwartz, J. Shabanowitz, D.F. Hunt, Int. J. Mass Spectrom. 236 (2004) 33.
[10] B.J. Engel, P. Pan, G.E. Reid, J.M. Wells, S.A. McLuckey, Int. J. Mass Spectrom. 219 (2002) 171.
[11] G.E. Reid, J. Wu, P.A. Chrisman, J.M. Wells, S.A. McLuckey, Anal. Chem. 73 (2001) 3274.
[12] J.M. Hogan, S.A. McLuckey, J. Mass Spectrom. 38 (2003) 245.
[13] P.A. Chrisman, S.J. Pitteri, J.M. Hogan, S.A. McLuckey, J. Am. Soc. Mass Spectrom. 16 (2005) 1020.
[14] J. Liu, Y. Xia, X.R. Liang, S.A. McLuckey, Proceedings of the 55th American Society for Mass Spectrometry, Indianapolis, IN, June 3, 2007.
[15] H.L. Han, Y. Xia, S.A. McLuckey, Rapid Commun. Mass Spectrom. 21 (2007) 1567.
[16] Y. Xia, H. Han, S.A. McLuckey, Anal. Chem. 80 (2008) 1111.
[17] D.L. Swaney, G.C. McAlister, M. Wirtala, J.C. Schwartz, J.E.P. Syka, J.J. Coon, Anal. Chem. 79 (2007) 477.
[18] K. Breuker, H.B. Oh, D.M. Horn, B.A. Cerda, F.W. McLafferty, J. Am. Chem. Soc. 124 (2002) 6407.
[19] F. Turecek, J. Am. Chem. Soc. 125 (2003) 5954.
[20] J.M. Wells, J.L. Stephenson, S.A. McLuckey, Int. J. Mass Spectrom. 203 (2000) A1.
[21] P.A. Chrisman, S.A. McLuckey, J. Proteome Res. 1 (2002) 549.
[22] J.L. Stephenson, B.J. Cargile, S.A. McLuckey, Rapid Commun. Mass Spectrom. 13 (1999) 2040.
[23] R.A. Zubarev, N.A. Kruger, E.K. Fridriksson, M.A. Lewis, D.M. Horn, B.K. Carpenter, F.W. McLafferty, J. Am. Chem. Soc. 121 (1999) 2857.
[24] H.P. Gunawardena, L. Gorenstein, D.E. Erickson, Y. Xia, S.A. McLuckey, Int. J. Mass Spectrom. 265 (2007) 130.
[25] M. Matsumura, G. Signor, B.W. Matthews, Nature 342 (1989) 291.
[26] T.E. Creighton, Bioessays 8 (1988) 57.

[27] J.M. Thornton, J. Mol. Biol. 151 (1981) 261.
[28] G.J. Van Berkel, K.G. Asano, P.D. Schnier, J. Am. Soc. Mass Spectrom. 12 (2001) 853.
[29] Y. Xia, P.A. Chrisman, D.E. Erickson, J. Liu, X.R. Liang, F.A. Londry, M.J. Yang, S.A. McLuckey, Anal. Chem. 78 (2006) 4146.
[30] X.R. Liang, Y. Xia, S.A. McLuckey, Anal. Chem. 78 (2006) 3208.
[31] Y. Xia, B.A. Thomson, S.A. McLuckey, Anal. Chem. 79 (2007) 8199.
[32] A. Loboda, A. Krutchinsky, O. Loboda, J. McNabb, V. Spicer, W. Ens, K. Standing, Eur. J. Mass Spectrom. 6 (2000) 531.
[33] B.A. Thomson, C.L. Jolliffe, US Patent 5,847,386, 1998.
[34] Y. Xia, P.A. Chrisman, S.J. Pitteri, D.E. Erickson, S.A. McLuckey, J. Am. Chem. Soc. 128 (2006) 11792.
[35] J.M. Wells, P.A. Chrisman, S.A. McLuckey, J. Am. Chem. Soc. 123 (2001) 12428.
[36] B.A. Budnik, Y.O. Tsybin, P. Hakansson, R.A. Zubarev, J. Mass Spectrom. 37 (2002) 1141.
[37] E.A. Syrstad, F. Turecek, J. Am. Soc. Mass Spectrom. 16 (2005) 208.
[38] I. Anusiewicz, M. Jasionowski, P. Skurski, J. Simons, J. Phys. Chem. A 109 (2005) 11332.
[39] M. Sobczyk, W. Anusiewicz, J. Berdys-Kochanska, A. Sawicka, P. Skurski, J. Simons, J. Phys. Chem. A 109 (2005) 250.